Matter Backreaction on Spin-Foam Hinges: Fermion Determinants, Regge Deficits, and Chiral Curvature Flow

Ginanjar Utama
ginanjar.utama@gmail.com

June 28, 2026

Abstract

The preceding paper in this sequence connected matter-first spin networks to the simplicity-constrained EPRL vertex: matter-line frames generate spacetime-algebra bivectors, the EPRL map selects a ray in the bivector invariant plane, and the Lorentzian four-simplex amplitude can be evaluated as a finite-cutoff tensor network on K_5. That result was kinematical and vertex-local. This paper asks the next question: when curvature is present, can the matter determinant see it, and can it back-react on the spin-foam flatness tendency? We build a finite hinge-link model in which several four-simplices meet around an internal triangle. The Regge deficit $\epsilon_h = 2\pi - \sum_{\sigma \supset h} \Theta_h^\sigma$ is represented as a rotation in the two-plane normal to the hinge, with spin lift $U_{\rm spin}(\epsilon_h)$. The first exact result is the holonomy obstruction

$$\det(I - U_{\rm spin}) = 16 \sin^4(\epsilon_h/4),$$

which vanishes in the flat sector, modulo the expected spinorial 4π periodicity. A finite graph Dirac operator on the hinge link reproduces the same obstruction and develops a curvature-induced spectral gap. Integrating out fermions therefore suppresses the near-flat zero-mode sector in a one-hinge toy model, opposing the gravitational flatness preference. For two hinges, disconnected link graphs factorise exactly, whereas edge-sharing link graphs have a non-zero determinant interaction; matter propagation then induces a curvature-curvature correlation between neighbouring defects. Finally we add a chiral $\mathrm{Spin}(4) = \mathrm{SU}(2)_+ \times \mathrm{SU}(2)_-$ split. A single finite hinge determinant is phase-trivial, $\arg\det(D_\chi + m) = 0$, so it can bias chiral variances but cannot by itself generate orientation-sign flow. The parity-odd channel in four dimensions is instead the Pontryagin pairing $\mathrm{tr}(\gamma_5 \Sigma_1 \Sigma_2) \sim B_1 \wedge B_2$, non-zero only for transverse hinge planes. The result is not a continuum limit or a derivation of the full spin-foam measure. It is a controlled finite-complex mechanism: fermion determinants are holonomy-sensitive functionals of Regge deficits and can induce matter-mediated curvature correlations on spin-foam hinge links.

1 Introduction

A matter-first programme for loop quantum gravity begins with interaction events and matter-line segments rather than a pre-existing lattice of geometry. Local spinor frames are attached to matter lines; comparing neighbouring frames defines a discrete connection; and loop curvature is recovered from the holonomy of those frame comparators. In the spacetime-algebra language, the elementary objects are bivectors: planes of rotation, boosts, areas, and curvature. A companion paper developed the first spin-foam bridge for this construction [2]: the EPRL simplicity constraint was identified as a ray in the bivector invariant plane, closure was shown to be equivalent to intertwiner admissibility, and the finite-cutoff Lorentzian EPRL four-simplex vertex was written as a tensor-network contraction on K_5.

That bridge was intentionally local. It explained how matter-built boundary data can enter one spin-foam vertex, but it did not answer the dynamical question that makes matter-first gravity interesting: once curvature is present, does the matter determinant see it, and can it back-react on the geometry selected by the spin-foam amplitude?

On a single flat four-simplex the answer is limited. A constant-tetrad fermion loop reduces to a volume contribution,

$$\Gamma_{\text{matter}} = V_4\, \rho_{\text{vac}}(m), \tag{1}$$

so the matter sector sees the determinant of the tetrad while the spin-foam sector sees the same tetrad through its triangle bivectors and area-angle Regge functional. This is useful but not yet curvature. In Regge calculus, curvature in four dimensions is concentrated on two-dimensional hinges: triangles around which several four-simplices meet. If the sum of dihedral angles around a hinge differs from 2π, the deficit angle

$$\epsilon_h = 2\pi - \sum_{\sigma \supset h} \Theta_h^\sigma \tag{2}$$

is the discrete curvature.

This paper promotes the matter-first determinant from the flat-cell setting to a curved hinge-link setting. The guiding picture is simple. Around a hinge, the normal 2-plane rotates by the Regge deficit. Spinors transported around the same loop pick up the spin lift of that rotation. Therefore a fermion determinant defined on the hinge-link graph cannot be blind to curvature.

The paper has four main claims.

1. **Curvature as spin holonomy.** A hinge with deficit ϵ_h has vector holonomy $U_{\text{vec}} = \exp(\epsilon_h B_h)$ in the normal plane and spin holonomy $U_{\text{spin}} = \exp(\epsilon_h \Sigma_h)$, with the half-angle periodicity of spinors. The determinant obstruction

$$\det(I - U_{\text{spin}}) = 16 \sin^4(\epsilon_h/4) \tag{3}$$

   vanishes only at flatness.

2. **A finite graph Dirac realises the obstruction.** On the ring graph linking the hinge, a dressed cyclic transfer operator satisfies $T^N = I \otimes U_{\text{spin}}(\epsilon_h)$. Its graph Dirac operator has a zero mode in the flat sector and a spectral gap proportional to the deficit.

3. **Matter back-reacts on flatness and couples hinges.** Since the massive fermion determinant is smallest near the flat zero-mode sector, integrating out fermions in a one-hinge model shifts probability away from exact flatness. For two hinges, disconnected link graphs factorise while edge-sharing link graphs have a non-zero determinant interaction, producing matter-induced curvature correlations.

4. **Chirality separates variance flow from orientation flow.** The $\text{Spin}(4) = \text{SU}(2)_+ \times \text{SU}(2)_-$ split gives a clean chiral handle on self-dual and anti-self-dual curvature. A single-hinge chiral determinant is real and phase-trivial, so it can bias the two chiral variances but cannot select an orientation sign. A true parity-odd directed term in four dimensions requires a Pontryagin channel $\text{tr}(\gamma_5 R \wedge R)$, represented at the discrete level by a transverse pair of hinge bivectors.

We use Euclidean Spin(4) for the finite determinant experiments, because the chiral split is clean and the numerical operators are finite-dimensional and well-conditioned. The Lorentzian spin-foam interpretation enters through the EPRL amplitude and its Regge asymptotics. The final section explains precisely what is exact, what is a finite model, and what remains to be done in a full EPRL multi-cell computation.

2 From flat tetrads to curved hinges

2.1 One tetrad, two sectoral functionals

Let a flat four-simplex be described by four edge vectors e_a from one vertex. Its proper volume is

$$V_4 = \frac{|\det(e_1, e_2, e_3, e_4)|}{4!}. \tag{4}$$

The same tetrad gives triangle areas through bivectors,

$$A_{ab} = \tfrac{1}{2}|e_a \wedge e_b|. \tag{5}$$

Thus a single tetrad feeds two sectoral functionals: the matter determinant through V_4, and the spin-foam/Regge sector through areas and dihedral angles.

For a constant flat cell the Euclidean Dirac determinant factorises as

$$\det_{\text{spinor}} (\mathrm{i}\gamma \cdot p + m) = (p^2 + m^2)^2, \tag{6}$$

and the one-loop effective action has the form (1). Since the cell is flat, the curvature heat-kernel coefficient vanishes. A volume-preserving shear of the tetrad can change the ten triangle areas while leaving V_4 fixed; the matter volume term is therefore not identical to the Regge area-angle functional.

The two sectoral functionals nevertheless co-vary under overall scale, which fixes the order at which the flat-cell determinant tracks the foam.

Proposition 1 (Volume–area–action co-variation)**.** *Under a homothety $e_a \mapsto s\,e_a$ one has $V_4 \mapsto s^4 V_4$, $A_{ab} \mapsto s^2 A_{ab}$, and the dihedral-weighted area sum $S_{\text{Regge}} = \sum_t A_t \Theta_t \mapsto s^2 S_{\text{Regge}}$ (the dihedral angles being scale-invariant). Hence*

$$\Gamma_{\text{matter}} \;\propto\; V_4 \;\propto\; A_t^2 \;\propto\; S_{\text{Regge}}^2. \tag{7}$$

A unit-Jacobian shear fixes V_4 (hence Γ_{matter}) while redistributing the individual areas.

Proof. V_4 is quartic and A_{ab} quadratic in the edge vectors, while Θ_t depends only on their directions; eliminating s^2 between the quadratic area and the quartic volume gives $V_4 \propto A_t^2 \propto S_{\text{Regge}}^2$. A unit-Jacobian map preserves $\det(e_1, \ldots, e_4)$, hence V_4, but need not preserve $|e_a \wedge e_b|$. □

The flat cell is the right control, but it cannot be the curvature test.

2.2 Regge curvature on a hinge

In four-dimensional Regge calculus, the elementary curvature support is a triangle h. If N four-simplices meet around h, the deficit is (2). Around that hinge the tangent plane to h is fixed, while the normal two-plane rotates by ϵ_h.

For a concrete scale we use the regular four-simplex, whose dihedral angle between tetrahedra meeting on a triangle is $\Theta = \arccos\frac{1}{4} = 1.31811\ldots$. Tiling N such cells around a hinge gives the representative deficits

$$\epsilon(N{=}3) = +2.329, \quad \epsilon(4) = +1.011, \quad \epsilon(5) = -0.307, \quad \epsilon(6) = -1.626, \tag{8}$$

so $N = 3, 4$ carry positive curvature and $N = 5, 6$ negative; the flat sector is $\epsilon = 0$.

Let (n_1, n_2) be an oriented orthonormal basis of the normal plane. The vector-representation generator is

$$B_h = n_2 \otimes n_1 - n_1 \otimes n_2, \qquad B_h^2 = -P_\perp, \tag{9}$$

where $P_\perp$ projects onto the normal plane. The vector holonomy is

$$U_{\text{vec}}(\epsilon_h) = \exp(\epsilon_h B_h). \tag{10}$$

It fixes the hinge plane and rotates the normal plane by ϵ_h.

For spinors we use Euclidean gamma matrices satisfying

$$\{\gamma_a, \gamma_b\} = 2\delta_{ab}, \qquad a, b \in \{0, 1, 2, 3\}, \qquad \gamma_5 = \gamma_0\gamma_1\gamma_2\gamma_3, \qquad \gamma_5^2 = I, \tag{11}$$

with all γ_a Hermitian; the same index range and chirality are used in the chiral split of Section 6. The spin generator in the same normal plane is

$$\Sigma_h = \frac{1}{4}[\gamma \cdot n_1, \gamma \cdot n_2], \tag{12}$$

and the spin holonomy is

$$U_{\text{spin}}(\epsilon_h) = \exp(\epsilon_h \Sigma_h). \tag{13}$$

The half-angle nature of spinors gives the characteristic 4π periodicity.

Proposition 2 (Hinge holonomy obstruction)**.** *For the four-component Dirac spinor representation of a rotation by deficit ϵ_h in a single normal two-plane,*

$$\det(I - U_{\text{spin}}(\epsilon_h)) = 16 \sin^4(\epsilon_h/4). \tag{14}$$

Thus the obstruction vanishes at flatness and is non-zero for a curved hinge modulo the expected spin-periodicity.

Proof. The spin representation decomposes into two identical two-dimensional normal-plane rotation blocks with eigenvalues $e^{\pm i\epsilon_h/2}$. Therefore

$$\det(I - U_{\text{spin}}) = (1 - e^{i\epsilon_h/2})^2(1 - e^{-i\epsilon_h/2})^2 = 16 \sin^4(\epsilon_h/4). \tag{15}$$

□

2.3 Heat-kernel curvature term

The same local geometry is the standard cone-times-hinge approximation. A small neighbourhood of a Regge hinge is approximated by

$$C_\alpha \times h, \qquad \alpha = 2\pi - \epsilon_h, \tag{16}$$

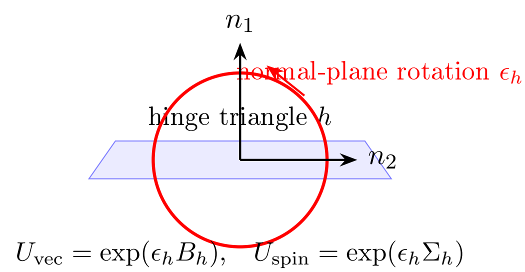

Figure 1: Curvature at a Regge hinge. The hinge plane is fixed; the normal plane rotates by the deficit ϵ_h. Spinors pick up the spin lift of the same holonomy.

where C_α is a two-dimensional cone in the normal plane and h is the hinge triangle. In this approximation the conical heat-kernel coefficient contains

$$C(\alpha) = \frac{1}{12}\left(\frac{2\pi}{\alpha} - \frac{\alpha}{2\pi}\right) = \frac{\epsilon_h}{12\pi} + O(\epsilon_h^2). \tag{17}$$

Multiplying by the hinge area gives a leading matter curvature contribution proportional to $A_h\epsilon_h$. This is the local Sakharov/Regge bridge: matter loops can induce the same hinge functional that appears in the Regge curvature term, although the coefficient and ultraviolet completion are regulator-dependent.

It is useful to place this against the standard continuum heat-kernel expansion of the one-loop effective action [13, 6],

$$\Gamma_{\text{eff}} = \int d^4x\,\sqrt{g}\left[c_0\,\Lambda_{\text{UV}}^4 + c_1\,\Lambda_{\text{UV}}^2\,R + c_2\,\log\!\Big(\frac{\Lambda_{\text{UV}}^2}{m^2}\Big)\mathcal{R}^2 + \cdots\right]. \tag{18}$$

The flat-cell determinant (1) is the discrete image of the volume term $c_0\Lambda_{\text{UV}}^4$, while the conical coefficient (17), weighted by the hinge area, is the local Regge analogue of the Einstein–Hilbert term $c_1\Lambda_{\text{UV}}^2 R$; the curvature-squared terms lie beyond the single-hinge model. This identification is heuristic — the discrete coefficients are regulator-dependent — but it fixes which continuum structure each finite object represents.

Remark 1 (Scope of the induced term). Equation (17) is a heat-kernel statement on the local product model (16). It is not a derivation of the full spin-foam measure and not yet a full discrete determinant on an arbitrary curved triangulation. The next sections replace this coefficient-level statement by explicit finite graph Dirac operators on hinge-link complexes.

3 A finite graph Dirac operator on the hinge link

3.1 The holonomy-transfer operator

The link of an internal hinge in the dual complex is a cycle graph C_N. Put a Dirac spinor at each of the N nodes and distribute the total spin holonomy uniformly along its edges. Let

$$g_N(\epsilon_h) = \exp(\epsilon_h \Sigma_h / N), \tag{19}$$

and let S be the cyclic shift on C_N. Define the dressed transfer operator

$$T(\epsilon_h, N) = S \otimes g_N(\epsilon_h). \tag{20}$$

Then

$$T^N = I_N \otimes U_{\rm spin}(\epsilon_h). \tag{21}$$

Proposition 3 (Finite graph realisation of the holonomy obstruction)**.** *For every ring size N,*

$$\det(I - T(\epsilon_h, N)) = \det(I - U_{\rm spin}(\epsilon_h)) = 16\sin^4(\epsilon_h/4). \tag{22}$$

The obstruction depends only on the total loop holonomy, not on how many cells resolve the loop.

Proof. If λ is an eigenvalue of $U_{\rm spin}$, then the corresponding eigenvalues of T are the N roots of λ. Hence

$$\prod_{\mu^N=\lambda} (1-\mu) = 1 - \lambda. \tag{23}$$

Multiplying over the spinor eigenvalues of $U_{\rm spin}$ gives the result. □

A simple anti-Hermitian graph Dirac operator is

$$D_{\rm hol}(\epsilon_h, N) = \frac{1}{2}(T - T^\dagger). \tag{24}$$

Its spectrum has a zero mode at flatness and a curvature-induced gap.

Proposition 4 (Curvature-induced graph gap)**.** *For the uniformly distributed hinge holonomy, the smallest absolute eigenvalue of $D_{\rm hol}$ is*

$$\min|\operatorname{spec} D_{\rm hol}| = \left|\sin\frac{\epsilon_h}{2N}\right|. \tag{25}$$

Thus the flat constant spinor is lifted by non-zero deficit.

Proof. The holonomy step $g_N = \exp(\epsilon_h \Sigma_h/N)$ has eigenvalues $e^{\pm i\epsilon_h/2N}$ on the two normal-plane spinor blocks, and the cyclic shift S has eigenvalues ω^k, $\omega = e^{2\pi i/N}$, $k = 0, \dots, N-1$. Hence $T = S \otimes g_N$ has eigenvalues $e^{i\phi_{k,\pm}}$ with phases $\phi_{k,\pm} = 2\pi k/N \pm \epsilon_h/2N$. For a unitary T, $\frac{1}{2}(T - T^\dagger)$ has eigenvalue $i\sin\phi$, so $-iD_{\rm hol}$ has the real spectrum $\{\sin\phi_{k,\pm}\}$. Its smallest modulus is attained at $k = 0$, giving $|\sin(\epsilon_h/2N)|$, which vanishes iff $\epsilon_h = 0$ within the local deficit branch under consideration. □

This gives the first finite determinant mechanism. For mass m, the integrated fermion contributes

$$Z_f(\epsilon_h) = |\det(D_{\rm hol}(\epsilon_h, N) + mI)|. \tag{26}$$

Since the determinant is smallest at flatness for small m, including it in the numerator suppresses the near-flat sector relative to a purely gravitational prior.

3.2 A one-hinge flatness toy

Let $\mu_{\rm grav}(\epsilon)$ be a positive local weight peaked at flatness. It may be a Gaussian prior or a local positive branch of the semiclassical Regge/EPRL factor $\cos(A_h\epsilon)$. Reweight it by the matter determinant:

$$P_s(\epsilon) = \frac{1}{Z_s}\,\mu_{\rm grav}(\epsilon)|\det(D_{\rm hol}(\epsilon, N) + mI)|^s, \tag{27}$$

where $s = +1$ represents integrating out Grassmann fermions and $s = -1$ represents a determinant in the denominator.

For $s = +1$, the flat zero-mode sector is relatively suppressed; the variance of ϵ grows and the probability near $\epsilon = 0$ falls. The distribution remains even: there is no sign preference $\langle\epsilon\rangle \neq 0$. This is not a solution of the spin-foam flatness problem, but it is a concrete finite mechanism by which fermions can oppose exact flatness.

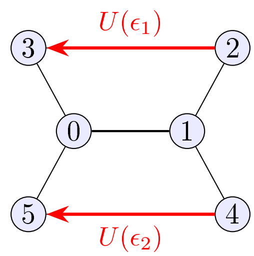

two hinge-link rings sharing edge $(0, 1)$

Figure 2: Two hinge-link rings sharing an edge. The shared graph support lets the fermion propagate between curvature defects, so the determinant need not factorise.

4 Two hinges and matter-mediated curvature coupling

A single hinge tests curvature sensitivity. A pair of hinges tests locality. If the matter determinant factorises over hinges, backreaction is local. If fermions can propagate from one hinge link to another through a shared part of the graph, the determinant can couple deficits.

Consider two ring graphs. In the disconnected control, the Dirac operator is a block direct sum:

$$D_{\text{dis}}(\epsilon_1, \epsilon_2) = D_1(\epsilon_1) \oplus D_2(\epsilon_2). \tag{28}$$

Then

$$\log|\det D_{\text{dis}}(\epsilon_1, \epsilon_2)| = \log|\det D_1(\epsilon_1)| + \log|\det D_2(\epsilon_2)|. \tag{29}$$

The interaction functional

$$\begin{aligned} I(\epsilon_1, \epsilon_2) = &\log|\det D(\epsilon_1, \epsilon_2)| - \log|\det D(\epsilon_1, 0)| \\ &- \log|\det D(0, \epsilon_2)| + \log|\det D(0, 0)| \end{aligned} \tag{30}$$

therefore vanishes exactly.

In the edge-sharing graph, two hinge rings share one graph edge. The determinant no longer factorises. Explicit finite matrices give $I \neq 0$ for generic deficits. Same-sign deficits raise $\log|\det|$ in the tested parameter range, while opposite signs flip the interaction sign.

Proposition 5 (Disconnected factorisation and shared-edge coupling)**.** *For two disconnected hinge-link graphs the determinant interaction* (30) *vanishes identically. For two hinge-link graphs sharing an edge, the same interaction is generically non-zero. Thus the fermion determinant is not local per hinge once fermion paths connect neighbouring hinge links.*

If the gravitational factor is approximated locally by the factorised branch

$$A_{\text{grav}}(\epsilon_1, \epsilon_2) = \cos(A_h \epsilon_1) \cos(A_h \epsilon_2), \tag{31}$$

then any connected correlation

$$\langle \epsilon_1 \epsilon_2 \rangle_c \tag{32}$$

in the positive local branch must be matter-induced. In finite scans the numerator fermion determinant gives a positive curvature correlation for edge-sharing hinges, while the inverse determinant flips the sign. The magnitude is model-dependent; the factorisation contrast is exact.

5 A genuine four-dimensional graph Dirac operator

The holonomy-transfer operator captures the loop obstruction, but it is not yet a four-dimensional Dirac operator in the sense of gamma matrices contracted with local normals. A closer finite analogue puts gamma matrices into the hopping term. Let the outward tetrahedral normal along the kth step of the hinge link be

$$\hat{n}_k = \cos(k\theta)n_1 + \sin(k\theta)n_2, \qquad \theta = \frac{2\pi - \epsilon}{N}. \tag{33}$$

Define

$$D_4(\epsilon, N)_{k,k+1} = \frac{1}{2}\gamma \cdot \hat{n}_k, \qquad D_4(\epsilon, N)_{k+1,k} = -\frac{1}{2}(\gamma \cdot \hat{n}_k)^\dagger, \tag{34}$$

with cyclic boundary conditions.

Proposition 6 (Chiral symmetry of the finite 4D hinge Dirac operator)**.** *The operator* (34) *is anti-Hermitian and anticommutes with* γ_5*:*

$$D_4^\dagger = -D_4, \qquad \{D_4, \gamma_5\} = 0. \tag{35}$$

Consequently the spectrum is γ_5*-symmetric, the massive vectorlike determinant* $\det(D_4 + m)$ *is real and even in the deficit, and a single hinge carries no parity-odd determinant phase.*

Proof. Anti-Hermiticity follows from the skew-symmetric placement of the hopping blocks. Since each $\gamma \cdot \hat{n}_k$ anticommutes with γ_5, so does the whole hopping operator, $\{D_4, \gamma_5\} = 0$. Hence if $D_4\psi = \mathrm{i}\lambda\psi$ then $D_4(\gamma_5\psi) = -\gamma_5 D_4\psi = -\mathrm{i}\lambda(\gamma_5\psi)$, so the spectrum of $-\mathrm{i}D_4$ is symmetric under $\lambda \mapsto -\lambda$, and $\det(D_4 + m) = \prod_{\lambda>0}(m^2 + \lambda^2) > 0$ is real, positive, and even in the deficit. □

This proposition is important because it prevents an overclaim. A genuine finite single-hinge Dirac determinant can see curvature through its magnitude, but it cannot produce orientation-sign flow by itself. In four dimensions the parity-odd curvature term is not an eta invariant of a one-dimensional hinge link. The relevant local object is the Pontryagin density $\mathrm{tr}(R \wedge R)$, which requires two independent curvature planes.

6 Chiral sectors and parity-odd curvature

6.1 The Spin(4) split

Euclidean spin curvature splits as

$$\mathrm{Spin}(4) \simeq \mathrm{SU}(2)_+ \times \mathrm{SU}(2)_-. \tag{36}$$

For a chosen orthonormal frame, a convenient pair of commuting generators is

$$J_+ = \tfrac{1}{2}(\Sigma_{01} - \Sigma_{23}), \qquad J_- = \tfrac{1}{2}(\Sigma_{01} + \Sigma_{23}), \tag{37}$$

where $\Sigma_{ab} = \frac{1}{4}[\gamma_a, \gamma_b]$. These act separately on the two γ_5 sectors. Deficits may therefore be organised as a pair (ϵ_+, ϵ_-), with parity represented by the swap

$$P : (\epsilon_+, \epsilon_-) \mapsto (\epsilon_-, \epsilon_+). \tag{38}$$

The chiral holonomy obstruction is the Weyl square root of the vectorlike obstruction:

$$\det(I - T_\pm) = 4\sin^2(\epsilon_\pm/4), \tag{39}$$

obtained from Proposition 3 restricted to a single Weyl sector, on which $J_\pm$ has eigenvalues $\pm\mathrm{i}/2$. Thus chiral matter can distinguish the two spin-curvature sectors: a vectorlike Dirac field uses both and is parity-even, whereas a one-sector chiral field can change which sector receives more curvature variance. The decisive question is whether this sectoral weighting can also choose an orientation sign. It cannot, and the obstruction is exact.

Proposition 7 (Phase-triviality of the one-hinge chiral determinant)**.** *Let $D_\chi = \frac{1}{2}(T_\chi - T_\chi^\dagger)$ be the chiral graph Dirac operator on the N-cell hinge link, with $T_\chi = S \otimes \exp(\epsilon J_\chi/N)$ and J_χ acting on one Weyl sector. Then for every $m > 0$ and every deficit ϵ,*

$$\arg\det(D_\chi + m) = 0, \qquad \det(D_\chi + m) \in \mathbb{R}_{>0}. \tag{40}$$

Proof. Since J_χ has eigenvalues $\pm\mathrm{i}/2$, the step holonomy $\exp(\epsilon J_\chi/N)$ has eigenvalues $e^{\pm\mathrm{i}\epsilon/2N}$, and $T_\chi = S \otimes \exp(\epsilon J_\chi/N)$ has eigenvalues $e^{\mathrm{i}\phi_{k,\pm}}$ with $\phi_{k,\pm} = 2\pi k/N \pm \epsilon/2N$, $k = 0, \ldots, N-1$. The Hermitian operator $-\mathrm{i}D_\chi$ then has the real spectrum $\{\sin\phi_{k,\pm}\}$. This multiset is symmetric under $\lambda \mapsto -\lambda$: for each $(k,\pm)$ the partner $k' = -k \bmod N$ with the opposite sign gives

$$\sin\Big(\tfrac{2\pi k'}{N} - \tfrac{\epsilon}{2N}\Big) = \sin\Big(-\tfrac{2\pi k}{N} - \tfrac{\epsilon}{2N}\Big) = -\sin\Big(\tfrac{2\pi k}{N} + \tfrac{\epsilon}{2N}\Big), \tag{41}$$

and as k runs over $\mathbb{Z}/N$ so does $-k$. Pairing eigenvalues $\{\lambda, -\lambda\}$,

$$\det(D_\chi + m) = \prod_\lambda (m + \mathrm{i}\lambda) = \prod_{\lambda>0} (m + \mathrm{i}\lambda)(m - \mathrm{i}\lambda) = \prod_{\lambda>0} (m^2 + \lambda^2) > 0. \tag{42}$$

□

Corollary 1 (Variance, not orientation)**.** *Because each chiral determinant is real, positive, and even in its deficit, weighting the two sectors by $|\det(D_{\chi,\pm} + m)|$ can induce a nonzero sectoral variance imbalance $\mathrm{Var}(\epsilon_+) - \mathrm{Var}(\epsilon_-) \neq 0$ while keeping $\langle\epsilon_\pm\rangle = 0$. A single hinge therefore supports chiral-sector variance flow but never an orientation-sign flow; a directed parity-odd term must enter through a separate spectral-asymmetry channel.*

This is the exact statement promised in the introduction. It complements the genuine four-dimensional operator of Proposition 6: there phase-triviality followed from $\{D_4, \gamma_5\} = 0$, here from the explicit $\lambda \mapsto -\lambda$ symmetry of the Weyl spectrum. Either way, the finite one-hinge chiral determinant is provably phase-trivial.

6.2 Pontryagin pairing of two hinge curvatures

The parity-odd four-dimensional curvature scalar is the Pontryagin density [17, 16]. In the finite hinge setting its local algebraic representative is the trace

$$P_{12} = \mathrm{tr}(\gamma_5 \Sigma_1 \Sigma_2), \tag{43}$$

where Σ_i is the spin generator associated with hinge i. If hinge i has oriented orthonormal normal-plane basis (p_i, q_i), then $\Sigma_i = \frac{1}{4}[\gamma \cdot p_i, \gamma \cdot q_i] = \frac{1}{2}(\gamma \cdot p_i)(\gamma \cdot q_i)$, and using the parity-odd Clifford trace

$$\mathrm{tr}(\gamma_5\, \gamma_a \gamma_b \gamma_c \gamma_d) = +4\, \epsilon_{abcd} \tag{44}$$

one finds

$$P_{12} = \epsilon_{abcd}\, p_1^a q_1^b p_2^c q_2^d = (p_1 \wedge q_1) \wedge (p_2 \wedge q_2) \;\sim\; B_1 \wedge B_2. \tag{45}$$

Since rotating either basis within its own plane leaves the unit bivector $p_i \wedge q_i$ fixed, P_{12} is a basis-independent geometric invariant of the ordered plane pair. This immediately gives a selection rule.

Proposition 8 (Transversality selection rule)**.** *The pairing $P_{12} = \mathrm{tr}(\gamma_5 \Sigma_1 \Sigma_2)$ vanishes whenever the two hinge normal planes fail to span $\mathbb{R}^4$, and is non-zero with sign equal to the handedness of the ordered pair when they are transverse. In particular, two hinges sharing an edge have $P_{12} = 0$.*

Proof. By (45), $P_{12} = (p_1 \wedge q_1) \wedge (p_2 \wedge q_2) \in \Lambda^4\mathbb{R}^4$ is the 4×4 determinant of the spanning vectors (p_1, q_1, p_2, q_2) times the volume form. It vanishes iff those four vectors are linearly dependent, i.e. iff the two planes fail to span $\mathbb{R}^4$, and otherwise equals (up to sign) the oriented volume, whose sign is the handedness. Two triangles sharing an edge both contain the edge direction in their tangent planes, so both *normal* planes lie in the three-dimensional orthogonal complement of that direction; two 2-planes inside a common 3-space always intersect in a line and cannot be transverse, hence $B_1 \wedge B_2 = 0$. □

For the regular four-simplex this is sharp. Two triangles sharing an edge, e.g. (012) and (013), give $P_{12} = 0$ exactly; a transverse pair sharing only a vertex, e.g. (012) and (234), has normal planes spanning $\mathbb{R}^4$ and yields $P_{12} = (p_1 \wedge q_1) \wedge (p_2 \wedge q_2) \approx -0.745$, with the opposite ordering $(012), (034)$ giving $+0.745$ — the same magnitude with reversed handedness.

The induced parity-odd term may then be modelled locally as

$$S_{\mathrm{odd}} = \mu\, \epsilon_1 \epsilon_2 P_{12}, \tag{46}$$

where μ is a chiral coupling. The sign of the induced curvature correlation is set by μP_{12} and flips under chirality reversal. This is the clean four-dimensional replacement for a single-hinge eta phase.

Remark 2 (Eta versus Pontryagin). A finite one-hinge chiral determinant is phase-trivial in the present four-dimensional model. Therefore an eta-like phase inserted as a one-variable function of ϵ should be treated as an ansatz, not as a derived determinant phase. The derived local parity-odd structure in four dimensions is the Pontryagin pairing of two transverse curvature planes.

7 Relation to the EPRL amplitude and the flatness problem

The EPRL vertex amplitude on non-degenerate Regge boundary data has a large-spin asymptotic structure involving the Regge action. For an internal hinge in a larger complex the relevant phase contains an area-deficit contribution

$$S_{\mathrm{Regge}} \supset A_h \epsilon_h. \tag{47}$$

The local two-saddle form is schematically

$$A_{\mathrm{grav}}(\epsilon_h) \sim \cos(A_h \epsilon_h + \varphi_h), \tag{48}$$

with phases and prefactors depending on the full boundary state. The simplified positive-branch experiments in this paper use this Regge/EPRL structure as a local semiclassical gravitational weight, not as a full booster-dressed multi-cell amplitude.

The flatness problem arises because spin-foam stationary phase conditions can impose unexpectedly strong restrictions on deficit angles in certain regimes [10, 11]. The determinant mechanisms here do not solve that problem. They show how matter could change the local effective weight:

$$W_{\mathrm{eff}}(\epsilon) \sim A_{\mathrm{grav}}(\epsilon)\, \det(D(\epsilon) + m)^s. \tag{49}$$

For $s = +1$ the fermion determinant suppresses the flat zero-mode sector in the finite hinge-link model. For edge-sharing hinge links it also generates correlations between neighbouring deficits. For chiral sectors it can distinguish self-dual and anti-self-dual curvature channels, while genuine parity-odd orientation flow requires the Pontryagin channel.

Module-level object	Exact content	Interpretation
Flat cell tetrad	$\Gamma_{\text{matter}} = V_4 \rho_{\text{vac}}$	matter sees volume only
Hinge holonomy	$\det(I - U_{\text{spin}}) = 16 \sin^4(\epsilon/4)$	curvature lifts spinor holonomy obstruction
Hinge-link graph Dirac	$T^N = I \otimes U_{\text{spin}}$; gap $\lvert \sin(\epsilon/2N) \rvert$	finite determinant is curvature-sensitive
Two edge-sharing hinges	disconnected factorises; shared-edge determinant does not	matter mediates curvature-curvature coupling
4D gamma-hopping Dirac	$\{D_4, \gamma_5\} = 0$; $\arg\det(D_\chi + m) = 0$	no one-hinge orientation phase
Transverse chiral pair	$P_{12} = \mathrm{tr}(\gamma_5 \Sigma_1 \Sigma_2) \neq 0$	parity-odd curvature channel

Table 1: Summary of finite-complex results and their interpretation.

8 Discussion

The previous paper established the bridge from matter-built boundary data to the simplicity-constrained EPRL vertex. This paper moves the matter-first programme from boundary kinematics to curvature and backreaction. The central point is that a fermion determinant on a hinge-link complex is not merely a volume factor. Once a loop holonomy is present, the determinant becomes a function of the Regge deficit.

Several results are exact within the finite models. The spin holonomy obstruction (14) follows directly from the spin representation of a normal-plane rotation. The graph-transfer operator reproduces that obstruction independently of the number of ring nodes. The disconnected two-hinge determinant factorises exactly, while the edge-sharing determinant is generically interacting. The gamma-hopping four-dimensional graph Dirac operator anticommutes with γ_5, which proves that the one-hinge chiral determinant is phase-trivial. The Pontryagin pairing selection rule follows from the Clifford trace with γ_5.

Other parts are deliberately model-level. The one-hinge backreaction probability uses a local positive gravitational weight rather than the full oscillatory spin-foam path integral. The two-hinge correlation uses a local semiclassical Regge/EPRL factor, not a full multi-cell EPRL amplitude with internal spin sums. The induced parity-odd term $S_{\text{odd}} = \mu \epsilon_1 \epsilon_2 P_{12}$ captures the correct handedness and selection rule, but its coefficient is regulator- and matter-content dependent. These limitations are not defects; they are the boundary between exact finite algebra and the still-open spin-foam continuum problem.

The next rigor upgrade is clear. One should construct a full finite simplicial Dirac operator on a curved four-dimensional complex, with edge lengths, dual volumes, and spin connections determined by simplex frames, then compare

$$\Delta \log |\det D| \quad \text{against} \quad \sum_h A_h \epsilon_h \tag{50}$$

across families of triangulations. In parallel, the gravitational weight should be replaced by the actual booster-dressed EPRL amplitude on the same multi-cell complex, including internal spin and intertwiner sums. Only then can one decide whether the matter-induced anti-flatness and curvature-correlation mechanisms survive in the full spin-foam model.

The broader lesson is nevertheless already visible. Matter does not simply sit on a background geometry. In a relational graph description, matter lines carry the frames whose mismatches define curvature. Their determinants are functions of the same loop holonomies that encode Regge deficits. Once curvature defects share graph support, fermions mediate interactions between those defects. And once chirality is included, the self-dual and anti-self-dual sectors can be weighted differently, with parity-odd structure controlled by the Pontryagin pairing of transverse hinge curvatures. The chiral $J_\pm$ split is the simplicial shadow of the self-dual/anti-self-dual decomposition underlying the Barbero–Immirzi parameter and the Holst term [15, 8], and the pairing (43) is the discrete analogue of the Nieh–Yan/Holst parity density [16]; a dynamically nonzero $\langle \epsilon_1 \epsilon_2 \rangle$ on transverse hinges would realise a spontaneously generated parity-odd gravitational coupling whose handedness is fixed by the matter chirality.

This is the matter-first slogan in finite-complex form: matter talks to matter; when the conversation closes around cycles, geometry appears; when the cycles are curved, the matter determinant talks back.

Acknowledgements

The author thanks the loop-quantum-gravity, Regge-calculus, geometric-algebra, spin-foam, and spectral-geometry communities whose tools make this bridge possible. Any errors in the finite models or their interpretation are the author's responsibility.

References

[1] G. Utama, "Matter-First Dynamics in LQG: Fermion Determinants, Spacetime-Algebra Tetrads, and an Induced Discrete Field Equation," ai.viXra.org:2606.0064 (2026), https://ai.vixra.org/abs/2606.0064.

[2] G. Utama, "Matter-First Spin Foams: Bivector Simplicity, Lorentzian Boosters, and a Tensor-Network EPRL Vertex," ai.viXra.org:2606.0074 (2026), https://ai.vixra.org/abs/2606.0074.

[3] R. Penrose, "Angular momentum: an approach to combinatorial spacetime," in *Quantum Theory and Beyond*, ed. T. Bastin (Cambridge University Press, 1971), pp. 151–180.

[4] M. Altaisky, "Combinatorial spacetime from loop quantum gravity," arXiv:2602.08341 [gr-qc] (2026).

[5] T. Regge, "General relativity without coordinates," Nuovo Cim. **19**, 558 (1961).

[6] A. D. Sakharov, "Vacuum quantum fluctuations in curved space and the theory of gravitation," Sov. Phys. Dokl. **12**, 1040 (1968).

[7] J. Engle, E. Livine, R. Pereira, and C. Rovelli, "LQG vertex with finite Immirzi parameter," Nucl. Phys. B **799**, 136 (2008).

[8] C. Rovelli and F. Vidotto, *Covariant Loop Quantum Gravity* (Cambridge University Press, 2014).

[9] J. W. Barrett, R. J. Dowdall, W. J. Fairbairn, F. Hellmann, and R. Pereira, "Lorentzian spin foam amplitudes: graphical calculus and asymptotics," Class. Quantum Grav. **27**, 165009 (2010).

[10] V. Bonzom, "Spin foam models for quantum gravity from lattice path integrals," Phys. Rev. D **80**, 064028 (2009).

[11] F. Hellmann and W. Kaminski, "Holonomy spin foam models: asymptotic geometry of the partition function," JHEP **10**, 165 (2013).

[12] D. V. Fursaev and S. N. Solodukhin, "On the description of the Riemannian geometry in the presence of conical defects," Phys. Rev. D **52**, 2133 (1995).

[13] D. V. Vassilevich, "Heat kernel expansion: user's manual," Phys. Rept. **388**, 279 (2003).

[14] M. F. Atiyah, V. K. Patodi, and I. M. Singer, "Spectral asymmetry and Riemannian geometry I," Math. Proc. Camb. Phil. Soc. **77**, 43 (1975).

[15] S. Holst, "Barbero's Hamiltonian derived from a generalized Hilbert–Palatini action," Phys. Rev. D **53**, 5966 (1996).

[16] H. T. Nieh and M. L. Yan, "An identity in Riemann–Cartan geometry," J. Math. Phys. **23**, 373 (1982).

[17] T. Eguchi, P. B. Gilkey, and A. J. Hanson, "Gravitation, gauge theories and differential geometry," Phys. Rept. **66**, 213 (1980).

[18] D. Hestenes, *Space-Time Algebra* (Gordon and Breach, 1966).

[19] C. Doran and A. Lasenby, *Geometric Algebra for Physicists* (Cambridge University Press, 2003).